

Optomechanical Cavity with a Buckled Mirror

D. Yuvaraj, M. B. Kadam, Oleg Shtempluck, and Eyal Buks
Department of Electrical Engineering, Technion, Haifa 32000 Israel

(Dated: July 5, 2012)

We study an optomechanical cavity, in which a buckled suspended beam serves as a mirror. The mechanical resonance frequency of the beam obtains a minimum value near the buckling temperature. Contrary to the common case, in which self-excited oscillations of the suspended mirror are optically induced by injecting blue detuned laser light, in our case self-excited oscillations are observed with red detuned light. These observations are attributed to a retarded thermal (i.e. bolometric) force acting on the buckled mirror in the inwards direction (i.e. towards to other mirror). With relatively high laser power other interesting effects are observed including period doubling of self-excited oscillations and intermode coupling.

PACS numbers: 46.40.-f, 05.45.-a, 65.40.De, 62.40.+i

I. INTRODUCTION

Systems combining mechanical elements in optical resonance cavities are currently a subject of intense interest [1–6]. Coupling of nanomechanical mirror resonators to optical modes of high-finesse cavities mediated by the radiation pressure has a promise of bringing the mechanical resonators into the quantum realm [2, 4, 7–13] (see Ref. [14] for a recent review). In addition, the micro-optoelectromechanical systems (MOEMS) are expected to play an increasing role in optical communications [15] and other photonics applications [16–18].

Besides the radiation pressure, another important force that contributes to the optomechanical coupling in MOEMS is the bolometric force [3, 19–24, 24, 25], also known as the thermal force. This force can be attributed to the heat induced deformations of the micromechanical mirrors [21–23, 26]. In general, the thermal force plays an important role in relatively large mirrors, in which the thermal relaxation rate is comparable to the mechanical resonance frequency. Phenomena such as mode cooling and self-excited oscillations [6, 23, 24, 27–31] have been shown in systems in which this force is dominant [3, 19, 24, 26, 32, 33].

In this paper we investigate an optomechanical cavity having a suspended mirror in the shape of a trilayer metallic doubly clamped beam [34–36]. The system experimentally exhibits some unusual behaviors. For example, contrary to other experiments, in which self-excited oscillations of the mechanical resonator are optically induced when the cavity is blue detuned [37], here the same effect occurs for the case of red-detuned cavity. Moreover, the dependence of the mechanical resonance frequency on laser power is found to be non-monotonic [38]. These findings are attributed to optically induced thermal strain in the beam, which gives rise to compressive stress that may result in buckling [39–44]. Bagheri *et al.* [45] have recently reported the utilization of the buckling phenomenon to develop a non-volatile mechanical memory element in a similar optomechanical system (see also Ref. [46]).

We generalized the theoretical model that has been

developed in Ref. [32] to account for the effect of buckling [47, 48]. We find that close to buckling the effective thermal force acting on the beam can become very large, and consequently optomechanical coupling is greatly enhanced. Consequently, the threshold laser power needed for optically driving self-excited oscillations in the mirror can be significantly reduced. We show that the proposed theoretical model can account for some of the experimental results. On the other hand, some other experimental observations remain elusive. For example, self-modulation of self-excited oscillations is observed in some ranges of operation. Further theoretical study, which will reveal the complex structure of stability zones and bifurcations of the system [49], is needed in order to account for such findings.

II. EXPERIMENTAL SETUP

The experimental setup (see Fig. 1) is similar to the one employed in Ref. [33]. A fiber Bragg grating (FBG) [50–52] and a microlens [53] are attached to the end of a single mode fiber. The fiber can be accurately positioned using piezomotors. The system, which consists of doubly clamped suspended multilayer micromechanical beam and the optical fiber monitoring assembly, is located inside a cryostat maintained under typical pressure of 10^{-3} mbar and temperature of 77 K. Optical cavity is formed between the freely suspended beam oscillating parallel to the optical axis of the cavity and between either the FBG or the glass-vacuum interface at the tip of the fiber, as shown in Fig. 1(a).

The multilayer beam is fabricated by using bulk micro-machining process. A 200 nm thick Nb layer is coated on prefabricated silicon nitride membranes over silicon substrates using DC magnetron sputtering at working pressure of 5.2×10^{-3} torr and argon atmosphere. Patterning on the coated substrates is done using photolithography followed by a liftoff process, in which a 10 nm thick layer of Cr and a 30 nm thick layer of gold-palladium ($\text{Au}_{0.85}\text{Pd}_{0.15}$) is patterned on top of the Nb layer. Front electron cyclotron resonance (ECR) plasma etching of the

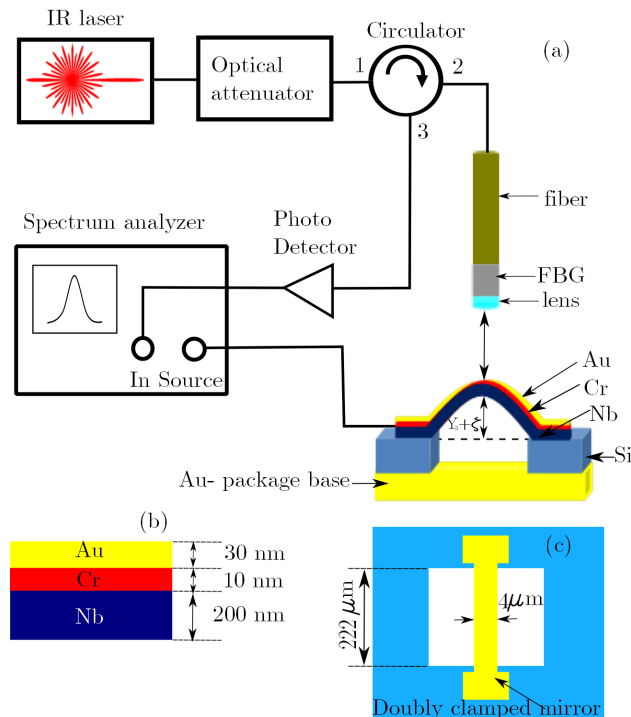


FIG. 1: The experimental setup. (a) Sample and optical displacement sensor. (b) Side view sketch of the trilayer beam mirror. (c) Top view of the suspended trilayer beam A.

unmasked Nb and silicon nitride is done to suspend the AuPd/Cr/Nb multilayer beam. Process is followed by a backside ECR plasma etching of the suspended beam to remove silicon nitride from back side. Figure 1(b) depicts the sketch of the multilayer AuPd/Cr/Nb suspended micro-mechanical beam having suspended length $l = 222 \mu\text{m}$, width $b = 4 \mu\text{m}$ and total thickness $h = 240 \text{ nm}$ with effective Young's modulus $E = 109.68 \times 10^9 \text{ Pa}$, density $\rho = 9715.22 \text{ kg/m}^3$, thermal expansion coefficient $\alpha = 7.76 \times 10^{-6} \text{ K}^{-1}$ and Poisson's ratio $\sigma = 0.3961$. These parameters are computed by averaging over the layers using expressions taken from Ref. [36]. The top view of the suspended trilayer beam mirror that is described in the following section is shown in Fig. 1(c). We will refer to this beam hereafter as beam A.

The suspended multilayer beam can be capacitively actuated by applying voltage to it with respect to the ground plate on which the sample is mounted. The ground plate is located at $500 \mu\text{m}$ below the suspended beam. Incident optical power is controlled by attenuating the injected laser power of wavelength $\lambda \simeq 1550 \text{ nm}$. The optical power reflected off the cavity is fed to a photodetector, which is monitored using a spectrum analyzer, as shown in Fig. 1(a).

III. SELF-EXCITED OSCILLATIONS INDUCED BY RED-DETUNED CAVITY

As was pointed out above, the optomechanical cavity under study exhibits some unusual behaviors. As is demonstrated in Fig. 2, self-excited oscillations can be induced by red-detuned cavity. Subplot (a) shows the reflected optical power vs. the voltage V_z , which is applied to the piezomotor that is used to position the optical fiber along the optical axis direction. The period of oscillation in the reflected power is $\lambda/2$. In this experiment the wavelength λ is not tuned to the reflective band formed by the FBG, and thus the optical cavity is formed between the freely suspended beam mirror and the glass-vacuum interface at the tip of the fiber. For this case the finesse of the cavity is much lower compared with values that can be achieved when the FBG is employed. Note that in addition to the oscillatory part, also the averaged (over one period of oscillation) measured reflected power exhibits dependence on cavity length [see subplot 2(a)]. The average value obtains a maximum when the cavity length coincides with the focal distance of the microlens. This occurs close to the value $V_z = 0$.

While the data seen in subplot 2(a) is taken when the input optical power is attenuated well below the threshold of self-excited oscillations, in subplot 2(b), which depicts the measured spectrum of reflected optical signal, the input power is set to 0.16 mW . Self excited oscillations of frequency of about 67 kHz are found near $V_z = 8 \text{ V}$ and near $V_z = 28 \text{ V}$. In both these regions where self excited oscillations occur the reflectivity decreases with V_z , i.e. the cavity is effectively red-detuned. As was discussed above, the deviation from periodic dependence of the measured spectrum on cavity length with $\lambda/2$ period is attributed to the effect of the microlens.

The dependence on laser power and P_L is seen in Fig. 3. The threshold power of self-excited oscillations occurs at 0.092 mW . In subplot 3(a) the static position y_0 of the center of beam A is measured vs. laser power below the threshold power. This is done by measuring the reflected optical power vs. the voltage V_z . For each value of the laser power this yield a plot similar to the one seen in Fig. 2(a). However, the phase of oscillations is found to depend on laser power. The value of the static deflection y_0 , which is extracted from that shift in the phase, is seen in subplot 3(a). The observed behavior indicates that the beam is deflected towards the optical fiber with increasing laser power. As will be seen below, this behavior indicates that the thermal force in the present case acts in the inwards direction, contrary to the more common situation (e.g. for the case of radiation pressure), where cavity optomechanical forces act in the outwards direction, and lead to elongation of the cavity (rather than shortening as in the current case).

In subplot 3(b) the mechanical resonance frequency f_0 is measured both below and above the threshold power of self-excited oscillations. While below the threshold of 0.092 mW the frequency f_0 is determined from forced

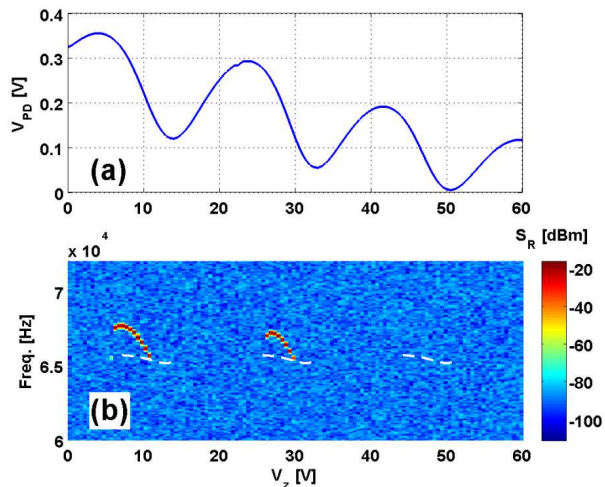


FIG. 2: (Color Online) Dependence on cavity length (beam A). (a) The photodetector DC voltage as a function of the voltage V_z applied to the piezomotor holding the fiber. A change of 18.5 V in V_z corresponds to a displacement of the fiber by $\lambda/2$. The laser power in this measurement is set to the value of 0.08 mW, which is lower than the threshold of self-excited oscillations. (b) Spectrum analyzer measurement of the photodetector voltage measured with a laser power of 0.16 mW. Self-excited oscillations are observed when the cavity is red-detuned. The white dotted line shows the calculated value of $\Omega_{\text{eff}}/2\pi$ for the regions in V_z for which $\gamma_{\text{eff}} < 0$. The following parameters have been used for the theoretical calculation $\theta_C = 0.06$, $\theta_f = 0.1$, $\Omega_0 = 1.2 \times 10^{-4}$, $\xi_C = 2.8 \times 10^{-3}$, $\gamma = 0.5 \times 10^{-9}$, $T_B = 0.96$, $T_A = 0.01$, $T_R = 0.6$, $\beta_Y = -1600$ and $\beta_{TR} = 2.6 \times 10^{-7}$.

oscillations (FO) (i.e. from the peak in the measured frequency response), above threshold f_0 is determined from the peak in the spectrum of self-excited oscillations (SO). Note the non-monotonic dependence of f_0 on laser power. As will be argued below, this dependence suggests that the beam undergoes thermal buckling.

IV. MECHANICAL EQUATIONS OF MOTION

Most of the experimental findings that were presented in the previous section are not accountable by the theoretical model that has been developed in Ref. [32] (which, on the other hand, was very successful in accounting for previous measurements of Ref. [33]). We therefore generalize the model to account for the effect of buckling in the mirror. While the derivation of the system's equations of motion is described in the appendices, the final equations are presented below in this section.

The height function $y(x, t)$ is assumed to have the shape of the first buckling configuration of a doubly clamped beam [47, 48]. Thus, for the case where the clamping points are located at $(x, y) = (\pm l/2, 0)$ the

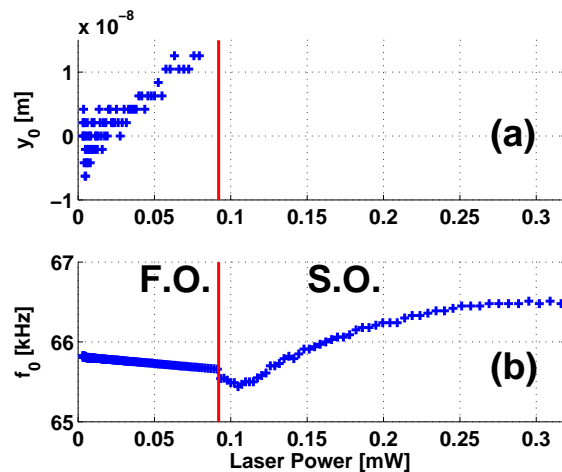


FIG. 3: Dependence of laser power (beam A). (a) The static deflection y_0 . (b) The mechanical frequency f_0 . The vertical red line represents the threshold of self-excited oscillations. Below the threshold f_0 is found from the peak amplitude of forced oscillations, whereas above the threshold f_0 is the frequency of self-excited oscillations.

height function $y(x, t)$ can be written as

$$y = \xi l \left(1 + \cos \frac{2\pi x}{l} \right), \quad (1)$$

where ξ depends on time. The equation of motion for ξ , which is derived in appendix C, is given by

$$\ddot{\xi} + 2\gamma\dot{\xi} + \Omega^2\xi = F_{\text{th}} + F_p e^{-i\Omega_p\tau}, \quad (2)$$

where overdot denotes a derivative with respect to the dimensionless time τ , which is related to the time t by the relation $\tau = t/\sqrt{\rho A_{\text{cs}}/E}$, where ρ is the mass density, A_{cs} is the cross section area of the beam, E is the Young's modulus, γ is the dimensionless damping constant, and F_p and Ω_p are the dimensionless amplitude and frequency respectively of an externally applied force. The equation of motion (2) contains two thermo optomechanical terms that depend on the temperature of the beam T . The first is the temperature dependent angular resonance frequency Ω and the second is the thermal force F_{th} . In terms of the dimensionless temperature $\theta = (T - T_0)/T_0$, where T_0 is the temperature of the supporting substrate (i.e. the base temperature) the frequency Ω is given by $\Omega = \Omega_0\nu(\theta)$, where $\Omega_0 = \sqrt{\rho A_{\text{cs}}/E}\omega_0$, ω_0 is the mode's angular resonance frequency and the temperature dependence is expressed in terms of the dimensionless function $\nu(\theta)$. The dimensionless thermal force is given by $F_{\text{th}} = \Omega^2\xi_C f_Y(\theta)$, where $\xi_C = \Omega_0\sqrt{3T_0(\alpha - \alpha_s)l^4/16\pi^6I}$, where α and α_s are the thermal expansion coefficients of the metallic beam and of the substrate respectively, I is the moment of inertia corresponding to bending in the xy plane, and the dimensionless function $f_Y(\theta)$ represents the beam's

temperature dependent deflection. For the case of a rectangular cross section having width l_y in the y direction and width l_z in the z direction, and for the case of bending in the xy plane I is given by $I = l_y^3 l_z / 12$. When small asymmetry is taken into account [see Eqs. (C3) and (C5)] the functions $f_Y(\theta)$ and $\nu(\theta)$ can be expressed as (see Fig. 6)

$$f_Y(\theta) = \text{Re} \left(\sqrt{\theta - \theta_C - i\theta_f} \right), \quad (3)$$

$$f_\nu^2(\theta) = -(\theta - \theta_C) + 3f_Y^2(\theta), \quad (4)$$

where θ_C is the dimensionless buckling temperature, which is related to the buckling temperature T_C by the relation $\theta_C = (T_C - T_0) / T_0$, and where the real dimensionless constant θ_f represents the effect of asymmetry.

V. OPTICAL CAVITY

The finesse of the optical cavity is limited by loss mechanisms that give rise to optical energy leaking out of the cavity. The main escape routes are through the on fiber mirror (FBG or glass-vacuum interface), through absorption by the metallic mirror, and through radiation; the corresponding transmission probabilities are respectively denoted by T_B , T_A and T_R . Let y_D be the displacement of the mirror relative to a point, at which the energy stored in the optical cavity in steady state obtains a local maximum. In the ideal case, all optical properties of the cavity are periodic in y_D with a period of $\lambda/2$, where λ is the optical wavelength (though, as can be seen in Fig. 2(a), deviation from periodic behavior is experimentally observed).

It is assumed that y_D is related to ξ by the following relation $4\pi y_D / \lambda = \beta_Y (\xi + \xi_f)$, where both β_Y and ξ_f are constants, which depend on the position of the fiber. For a fixed ξ the cavity reflection probability R_C , i.e. the ratio between the reflected (outgoing) and injected (incoming) optical powers in the fiber, is given by [33]

$$R_C = \frac{\left(\frac{T_B - T_A - T_R}{2}\right)^2 + 2[1 - \cos(\beta_Y(\xi + \xi_f))]}{\left(\frac{T_B + T_A + T_R}{2}\right)^2 + 2[1 - \cos(\beta_Y(\xi + \xi_f))]} . \quad (5)$$

The heating power Q due to optical absorption of the suspended micromechanical mirror can be expressed as $Q = I(\xi) P_L$, where P_L is the power of the monochromatic laser light incident on the cavity and where the function $I(\xi)$ is given by [33]

$$I(\xi) = \frac{T_B T_A}{\left(\frac{T_B + T_A + T_R}{2}\right)^2 + 2[1 - \cos(\beta_Y(\xi + \xi_f))]} . \quad (6)$$

VI. THERMAL BALANCE EQUATION

The temperature T evolves according to the following thermal balance equation

$$\frac{dT}{dt} = \frac{Q}{C} - \frac{H(T - T_0)}{C}, \quad (7)$$

where C is heat capacity, H is thermal transfer coefficient and Q is the heating power due to optical absorption. In terms of the dimensionless temperature θ and dimensionless time τ the thermal balance equation becomes

$$\dot{\theta} = \beta_P I(\xi) - \beta_{TR} \theta, \quad (8)$$

where $\beta_{TR} = \sqrt{\Upsilon/E} H / C$ is the dimensionless thermal rate, and $\beta_P = \sqrt{\Upsilon/E} P_L / C T_0$ is the dimensionless injected laser power.

VII. SMALL AMPLITUDE LIMIT

The coupling between the equation of motion for ξ [Eq. (2)] and the one for θ [Eq. (8)] origins by three terms, the θ dependent frequency Ω , the θ dependent force F_{th} (i.e. the thermal force) [see Eq. (2)], and the ξ dependent optical heating power [the term $I(\xi)$ in Eq. (8)]. The case where the first two coupling terms are linearized (i.e. approximated by a linear function of θ) is identical to the case that was studied in Ref. [32], in which slow envelope evolution equations for the system were derived, and the amplitudes and the corresponding oscillation frequencies of different limit cycles were analyzed. By employing the same analysis (and the same simplifying assumptions) for the present case one finds that the coupling leads to renormalization of the mechanical damping rate, which effectively becomes

$$\gamma_{\text{eff}} = \gamma + \frac{f'_Y I' \xi_C \beta_P}{2 \left(1 + \frac{\beta_{TR}^2}{\Omega^2}\right)}, \quad (9)$$

where $I' = dI/d\xi$ and where $f'_Y = df_Y/d\theta$. The corresponding effective mechanical resonance frequency Ω_{eff} is given by

$$\Omega_{\text{eff}} = \Omega - \frac{(\gamma_{\text{eff}} - \gamma) \beta_{TR}}{\Omega_p}. \quad (10)$$

The white dotted line in Fig. 2(b) shows the calculated value of Ω_{eff} [see Eq. (10)] for the regions in V_z for which $\gamma_{\text{eff}} < 0$ [see Eq. (9)]. The system's parameters that were used for the calculation are listed in the caption of Fig. 2. Note that Eqs. (9) and (10), which were derived by assuming the limit of small amplitudes, become inapplicable in most of the region, in which self-excited oscillations are observed in Fig. 2(b), and consequently, relatively large deviation between data and the prediction of Eq. (10) is expected.

The threshold of instability, i.e. Hopf bifurcation, occurs when γ_{eff} vanishes. For the case where the dominant coupling mechanism between the mechanical resonator and the optical field arises due to radiation pressure, instability can occur only for the so-called case of blue detuning, i.e. the case where $I' < 0$. However, contrary to the case of radiation pressure [37, 54], which always acts in the outwards direction, the thermal force due to buckling can act in both directions. We refer to the case where

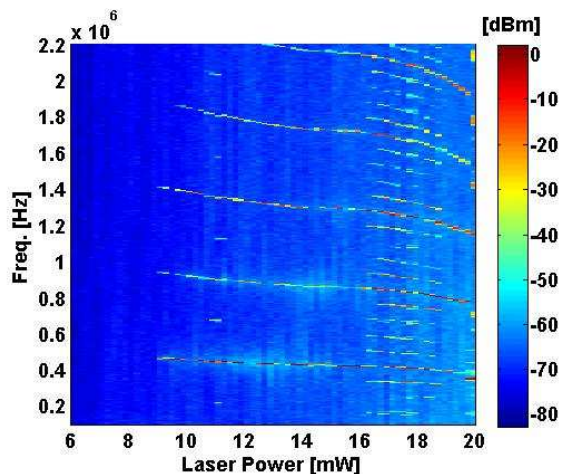


FIG. 4: (Color Online) In addition to the harmonics in the measured spectrum due to self-excited oscillations of mode 1 of beam B, subharmonics of order 1/2 and of order 1/5 are observed.

$f'_Y > 0$ as the case of outwards buckling, in which due to buckling the optical cavity becomes longer, whereas the opposite case of inwards buckling occurs when $f'_Y < 0$. As can be seen from Eq. (9), the threshold laser power β_P at which Hopf bifurcation occurs is inversely proportional to $|f'_Y|$. Close to the buckling temperature θ_C and when asymmetry is small (i.e. when $|\theta_f| \ll 1$) the factor $|f'_Y|$ can become very large [see Eq. (3) and Fig. 6], and consequently, the threshold laser power in that region can become very small.

VIII. HIGH LASER POWER

Other interesting effects have been observed with relatively high laser power. Two examples are presented below. The multilayer beam mirror that was used for the experiments that are introduced in this section (see Figs. 4 and 5) has the same layer structure as beam A [see Fig. 1(b)], however its length is $l = 120 \mu\text{m}$ and its width is $b = 20 \mu\text{m}$. We will refer to this beam hereafter as beam B. The same fabrication process has been employed for both beams. The two lowest lying modes of beam B, which are hereafter referred to as mode 1 and mode 2, have resonance frequencies f_1 and f_2 of about 510 kHz and 1200 kHz respectively (note that these values vary with laser power and cavity length).

Self-excited oscillations of mode 1 are seen in Fig. 4. In this measurement the sample is kept grounded and the reflected optical power is measured using a spectrum analyzer as a function of input optical power. In the frequency window that has been employed for this measurement the first 5 harmonics of the self-oscillating mode 1 are seen. In addition, for some values of input power the spectrum contains subharmonics. Close to input power

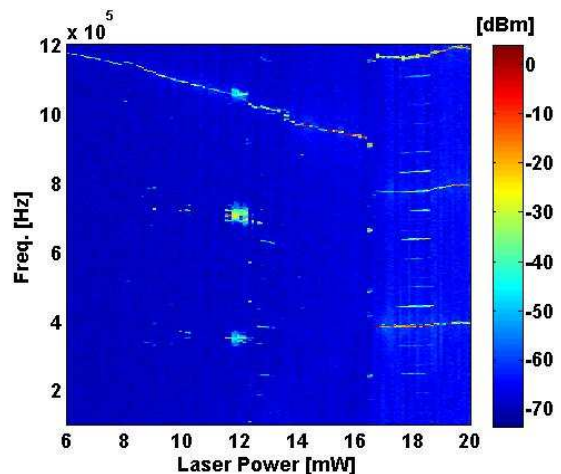


FIG. 5: (Color Online) The subharmonics of order 1/3 near input power of 11.9 mW are attributed to excitation of mode 1 by the self-oscillating mode 2, which has a frequency f_2 that is 3 times larger than f_1 in that region.

of 11 mW the subharmonics indicate that period doubling occurs, whereas in the range 16.2 – 18.6 mW the period is multiplied by a factor of 5. While the period doubling effect has been predicted for a similar system by Blocher *et al.* [49], the underlying mechanism responsible for the period multiplication by a factor of 5 is yet undetermined.

The data in Fig. 5, which was taken with a modified cavity length, exhibits self-excited oscillations of mode 2 in the laser input power range 6 – 16.5 mW. Above that range self-excited oscillations of mode 1 are observed. Near input power of 11.9 mW the ratio between f_2 and f_1 is 3, i.e. $f_2 = 3f_1$. This gives rise to strong intermode coupling, which leads to excitation of mode 1 by the self-oscillating mode 2, as can be seen from the subharmonics of order 1/3 that are measured in that range.

Note that for other cavity lengths the measured spectrum of reflected power can exhibit wide band response when the input laser power is sufficiently large. This possibly indicates that the dynamics becomes chaotic [49].

IX. SUMMARY

In summary, an optomechanical cavity having a buckled mirror may exhibit some unusual behaviors when the operating temperature is close to the buckling temperature. In that range the instability threshold can be reached with relatively low laser power. Moreover, contrary to the more common case, the instability is obtained with red detuned laser light for the case of inwards buckling. With relatively high laser power other interesting effects are observed in the unstable region including period doubling and intermode coupling. Further theoretical work is needed to account for such effects.

Both first authors (D. Y. and M. B. K.) have equally contributed to the paper.

Appendix A: Lagrangian

Consider a beam made of a material having mass density ρ and Young's modulus E . In the absent of tension the length of the beam is l_0 . The beam is doubly clamped to a substrate at the points $(x, y) = (\pm l/2, 0)$ and the motion of the beam's axis, which is described by the height function $y(x, t)$, is assumed to be exclusively in the xy plane. The corresponding moment of inertia is denoted by I . The Lagrangian functional \mathcal{L} is given by [48]

$$\mathcal{L} = \int_{-l/2}^{l/2} dx L - \frac{\beta_A E l}{8} \left(\int_{-l/2}^{l/2} dx \left(\frac{\partial y}{\partial x} \right)^2 \right)^2, \quad (\text{A1})$$

where

$$L = \frac{A_{cs}\rho}{2} \left(\frac{\partial y}{\partial t} \right)^2 - \frac{N}{2} \left(\frac{\partial y}{\partial x} \right)^2 - \frac{EI}{2} \left(\frac{\partial^2 y}{\partial x^2} \right)^2 + fy \quad (\text{A2})$$

is the Lagrangian density, A_{cs} is the cross section area of the beam and

$$N = EA_{cs} \frac{l - l_0}{l_0} \quad (\text{A3})$$

is the tension in the beam for the straight case where $y = 0$. The beam's equation of motion is found from the principle of least action to be given by [47]

$$\Upsilon \frac{\partial^2 y}{\partial t^2} = \left(N + \frac{A_{cs} E}{2l} \int_{-l/2}^{l/2} dx \left(\frac{\partial y}{\partial x} \right)^2 \right) \frac{\partial^2 y}{\partial x^2} - EI \frac{\partial^4 y}{\partial x^4} + f, \quad (\text{A4})$$

where $\Upsilon = \rho A_{cs}$ is the mass density per unit length.

Appendix B: First Buckling Configuration

Consider the case where the deflection $y(x, t)$ has the shape of the first buckling configuration [47], i.e. $y = \mathcal{Y}l \left(1 + \cos \frac{2\pi x}{l} \right)$, where \mathcal{Y} is a dimensionless time dependent amplitude. In order to account for a possible asymmetry, the force f is allowed to be a nonzero constant [44, 48]. The Lagrangian (A1) for the present case becomes

$$\mathcal{L}_0 = \frac{3\beta_A \rho l^5 \left(\frac{d\mathcal{Y}}{dt} \right)^2}{4} - \pi^2 N l \mathcal{Y}^2 - 4\pi^4 \beta_I E l^3 \mathcal{Y}^2 + f l^2 \mathcal{Y} - \frac{\pi^4 \beta_A E l^3 \mathcal{Y}^4}{2}, \quad (\text{B1})$$

where $\beta_A = A_{cs}/l^2$ and where $\beta_I = I/l^4$. Alternatively, \mathcal{L}_0 can be expressed as

$$\mathcal{L}_0 = T_0 - U_0, \quad (\text{B2})$$

where the kinetic energy T_0 is given by

$$T_0 = \frac{m_0 l^2 \left(\frac{d\mathcal{Y}}{dt} \right)^2}{2}, \quad (\text{B3})$$

where $m_0 = 3\beta_A \rho l^3/2$ and where the potential energy U_0 is given by

$$U_0 = \frac{m_0 \omega_0^2 l^2}{2} u(\mathcal{Y}), \quad (\text{B4})$$

where

$$u(\mathcal{Y}) = \eta_1 \mathcal{Y} + \eta_2 \mathcal{Y}^2 + \eta_4 \mathcal{Y}^4, \quad (\text{B5})$$

$\eta_1 = -2f/m_0 \omega_0^2$, $\eta_2 = 1 - \beta_L$, $\eta_4 = \pi^4 \beta_A E l / m_0 \omega_0^2$, $\beta_L = -N/4\pi^2 \beta_I E l^2$ and where $\omega_0^2 = (2\pi)^4 \beta_I E / 3\rho A_{cs}$.

Local minima points \mathcal{Y}_0 of the potential U_0 are found by solving $0 = du/d\mathcal{Y}$. The dimensionless potential $u(\mathcal{Y})$ can be expanded near one of its local minima points \mathcal{Y}_0 to second order in $\mathcal{Y} - \mathcal{Y}_0 \equiv \xi$ as $u = u_0 + \nu^2 \xi^2 + O(\xi^3)$, where both u_0 and $\nu = \sqrt{\eta_2 + 6\eta_4 \mathcal{Y}_0^2}$ are constants.

For the case where $\eta_1 = 0$ the coordinate \mathcal{Y}_0 is given by $\mathcal{Y}_0 = \pm \text{Re} \sqrt{-\eta_2/2\eta_4}$. The solution for the case of small $|\eta_1|$ can be approximated by

$$\mathcal{Y}_0 = \text{Re} \sqrt{-\frac{\eta_2 + i(4\eta_1^2 \eta_4)^{1/3}}{2\eta_4}}, \quad (\text{B6})$$

provided that $|\eta_2|$ is small, i.e. provided that the system is close to buckling conditions. The corresponding approximation for ν is found from the relation $\nu = \sqrt{\eta_2 + 6\eta_4 \mathcal{Y}_0^2}$.

Appendix C: Mechanical equation of motion

Let α and α_s be the thermal expansion coefficients of the metallic beam and of the substrate respectively. At some given temperature T_{TF} the tension N is assumed to vanish. Since the substrate is much larger than the beam, one may assume that the substrate thermally contracts (or expands) as if the suspended beam was not attached to it, namely the distance between both clamping points at temperature $T = T_{TF} + \Delta_T$ becomes $l_s = l_0 (1 + \alpha_s \Delta_T)$, where l_0 is the distance at the tension free temperature T_{TF} . The tension N needed to keep the beam clamped to the substrate is thus given by $N = EA_{cs} (\alpha_s - \alpha) \Delta_T$ [55]. Thus, the dimensionless parameter β_L can be expressed as a function of the dimensionless temperature

$$\theta = \frac{T - T_0}{T_0}, \quad (\text{C1})$$

where T_0 is the temperature of the supporting substrate (i.e. the base temperature), as $\beta_L = \beta_A \beta_{T_0} (\theta + \beta_{TF}) / 4\pi^2 \beta_I$ where $\beta_{T_0} = T_0 (\alpha - \alpha_s)$ and where $\beta_{TF} = (T_0 - T_{TF}) / T_0$. Alternatively, β_L can be expressed as

$$\beta_L = 1 + \frac{\beta_A \beta_{T_0} (\theta - \theta_C)}{4\pi^2 \beta_I}, \quad (C2)$$

where $\theta_C = 4\pi^2 \beta_I / \beta_A \beta_{T_0} - \beta_{TF}$ is the dimensionless temperature at which buckling occurs in the symmetric case (i.e. the case where $\eta_1 = 0$).

With the help of Eq. (C2) the parameters \mathcal{Y}_0 and ν can be expressed as a function of the dimensionless temperature θ . For the case of small asymmetry one has [see Eq. (B6)]

$$\mathcal{Y}_0 = \xi_C f_Y(\theta), \quad (C3)$$

where the function $f_Y(\theta)$ is given by Eq. (3), $\theta_f = 4\pi^2 \beta_I (4\eta_1^2 \eta_4)^{1/3} / \beta_A \beta_{T_0}$ and the coefficient ξ_C is given by

$$\xi_C = \sqrt{\frac{\beta_A \beta_{T_0}}{8\pi^2 \beta_I \eta_4}} = \sqrt{\frac{3T_0 (\alpha - \alpha_s) A_{cs} \rho l^4 \omega_0^2}{16\pi^6 EI}}. \quad (C4)$$

The corresponding approximation for ν is given by

$$\nu = \nu_C f_\nu(\theta), \quad (C5)$$

where

$$\nu_C = \sqrt{\frac{\beta_A \beta_{T_0}}{4\pi^2 \beta_I}} = \sqrt{\frac{A_{cs} l^2 T_0 (\alpha - \alpha_s)}{4\pi^2 I}}, \quad (C6)$$

and where the function $f_\nu(\theta)$ is given by Eq. (4). The functions $f_Y(\theta)$ and $f_\nu(\theta)$ are plotted in Fig. 6.

The temperature dependence of \mathcal{Y}_0 can be taken into account by adding a thermal force term F_{th} [40, 56, 57] to the equation of motion of the mechanical amplitude $\xi = \mathcal{Y} - \mathcal{Y}_0$. Similarly, the temperature dependence of

ν can be taken into account by including a thermal frequency shift term. When in addition damping and external driving are taken into account the equation of motion (2) for ξ is obtained.

Acknowledgment

We would like to thank Yuli Starosvetsky for many fruitful discussions and important comments. This work was supported by the German Israel Foundation under Grant No. 1-2038.1114.07, the Israel Science Foundation under Grant No. 1380021, the Deborah Foundation, the Mitchel Foundation, Ministry of Science, Russell Berrie Nanotechnology Institute, the European STREP QNEMS Project, MAGNET Metro 450 consortium and MAFAT.

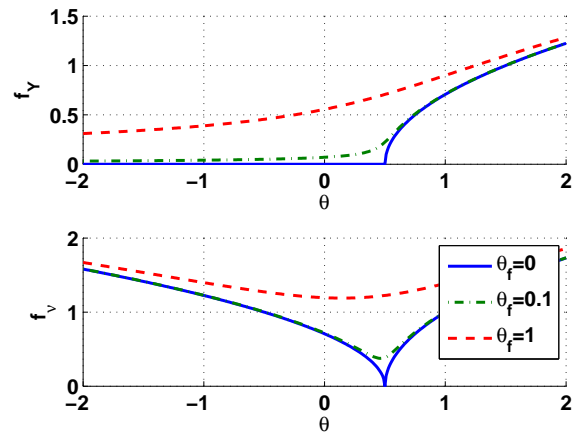


FIG. 6: (Color Online) The functions $f_Y(\theta)$ and $f_\nu(\theta)$ [see Eqs. (3) and (4)] plotted for 3 different values of the asymmetry parameter θ_f and for the case where the dimensionless buckling temperature is $\theta_C = 0.5$.

-
- [1] V. B. Braginsky and A. B. Manukin, “Ponderomotive effects of electromagnetic radiation (in Russian),” *ZhETF*, vol. 52, pp. 986–989, 1967.
- [2] S. Gigan, H. R. Böhm, M. Paternostro, F. Blaser, J. B. Hertzberg, K. C. Schwab, D. Bauerle, M. Aspelmeyer, and A. Zeilinger, “Self cooling of a micromirror by radiation pressure,” *Nature*, vol. 444, pp. 67–70, 2006.
- [3] C. H. Metzger and K. Karrai, “Cavity cooling of a microlever,” *Nature*, vol. 432, pp. 1002–1005, 2004.
- [4] T. J. Kippenberg and K. J. Vahala, “Cavity optomechanics: Back-action at the mesoscale,” *Science*, vol. 321, no. 5893, pp. 1172–1176, Aug 2008.
- [5] C. Metzger, I. Favero, S. Camerer, D. Konig, H. Lorenz, J. P. Kotthaus, and K. Karrai, “Optical cooling of a

micromirror of wavelength size,” *Appl. Phys. Lett.*, vol. 90, pp. 104101, 2007.

- [6] K. Hane and K. Suzuki, “Self-excited vibration of a self-supporting thin film caused by laser irradiation,” *Sensors and Actuators A: Physical*, vol. 51, pp. 179–182, 1996.
- [7] H. J. Kimble, Y. Levin, A. B. Matsko, K. S. Thorne, and S. P. Vyatchanin, “Conversion of conventional gravitational-wave interferometers into quantum non-demolition interferometers by modifying their input and/or output optics,” *Phys. Rev. D*, vol. 65, pp. 022002, Dec 2001.
- [8] T. Carmon, H. Rokhsari, L. Yang, T. J. Kippenberg, and K. J. Vahala, “Temporal behavior of radiation-pressure-induced vibrations of an optical microcavity

- phonon mode,” *Phys. Rev. Lett.*, vol. 94, pp. 223902, Jun 2005.
- [9] O. Arcizet, P.-F. Cohadon, T. Briant, M. Pinard, and A. Heidmann, “Radiation-pressure cooling and optomechanical instability of a micromirror,” *Nature*, vol. 444, pp. 71–74, Nov 2006.
- [10] A. M. Jayich, J. C. Sankey, B. M. Zwickl, C. Yang, J. D. Thompson, S. M. Girvin, A. A. Clerk, F. Marquardt, and J. G. E. Harris, “Dispersive optomechanics: a membrane inside a cavity,” *New J. Phys.*, vol. 10, pp. 095008, Sep 2008.
- [11] A. Schliesser, R. Riviere, G. Anetsberger, O. Arcizet, and T. J. Kippenberg, “Resolved-sideband cooling of a micromechanical oscillator,” *Nat. Phys.*, vol. 4, pp. 415–419, 2008.
- [12] C. Genes, D. Vitali, P. Tombesi, S. Gigan, and M. Aspelmeyer, “Ground-state cooling of a micromechanical oscillator: Comparing cold damping and cavity-assisted cooling schemes,” *Phys. Rev. A*, vol. 77, pp. 033804, Mar 2008.
- [13] J. D. Teufel, D. Li, M. S. Allman, K. Cicak, A. J. Sirois, J. D. Whittaker, and R. W. Simmonds, “Circuit cavity electromechanics in the strong coupling regime,” *arXiv*, Nov 2010.
- [14] Menno Poot and Herre S.J. van der Zant, “Mechanical systems in the quantum regime,” *Phys. Rep.*, vol. 511, pp. 273–335, 2012.
- [15] M. C. Wu, O. Solgaard, and J. E. Ford, “Optical MEMS for lightwave communication,” *J. Lightwave Technol.*, vol. 24, no. 12, pp. 4433–4454, Dec 2006.
- [16] N. A. D. Stokes, R. M. A. Fatah, and S. Venkatesh, “Self-excitation in fibre-optic microresonator sensors,” *Sens. Actuators A*, vol. 21, pp. 369–372, Feb 1990.
- [17] S.E. Lyshevski and M.A. Lyshevski, “Nano- and microoptoelectromechanical systems and nanoscale active optics,” in *Third IEEE Conference on Nanotechnology, 2003.*, Aug 2003, vol. 2, pp. 840–843.
- [18] M. Hossein-Zadeh and K. J. Vahala, “An optomechanical oscillator on a silicon chip,” *IEEE J. Sel. Top. Quantum Electron.*, vol. 16, no. 1, pp. 276–287, Jan 2010.
- [19] G. Jourdan, F. Comin, and J. Chevrier, “Mechanical mode dependence of bolometric backaction in an atomic force microscopy microlever,” *Phys. Rev. Lett.*, vol. 101, pp. 133904, Sep 2008.
- [20] F. Marino and F. Marin, “Chaotically spiking attractors in suspended mirror optical cavities,” *arXiv*, Jun 2010.
- [21] S. D. Liberato, N. Lambert, and F. Nori, “Quantum limit of photothermal cooling,” *arXiv*, Nov 2010.
- [22] M. Paternostro, S. Gigan, M. S. Kim, F. Blaser, H. R. Böhm, and M. Aspelmeyer, “Reconstructing the dynamics of a movable mirror in a detuned optical cavity,” *New J. Phys.*, vol. 8, pp. 107, Jun 2006.
- [23] F. Marquardt, J. G. E. Harris, and S. M. Girvin, “,” *Phys. Rev. Lett.*, vol. 96, pp. 103901, 2006.
- [24] C. Metzger, M. Ludwig, C. Neuenhahn, A. Ortlieb, I. Favero, K. Karrai, and F. Marquardt, “Self-induced oscillations in an optomechanical system driven by bolometric backaction,” *Phys. Rev. Lett.*, vol. 101, pp. 133903, Sep 2008.
- [25] J. Restrepo, J. Gabelli, C. Ciuti, and I. Favero, “Classical and quantum theory of photothermal cavity cooling of a mechanical oscillator,” *Comptes Rendus Physique*, vol. 12, pp. 860–870, Nov 2011.
- [26] K. Aubin, M. Zalalutdinov, T. Alan, R.B. Reichenbach, R. Rand, A. Zehnder, J. Parpia, and H. Craighead, “Limit cycle oscillations in CW laser-driven NEMS,” *J. Microelectromech. Syst.*, vol. 13, pp. 1018 – 1026, Dec 2004.
- [27] Kiwoong Kim and Soonchil Lee, “Self-oscillation mode induced in an atomic force microscope cantilever,” *J. Appl. Phys.* 91, 4715 (2002); doi:10.1063/1.1454225 (5 pages) *Self-oscillation mode induced in an atomic force microscope cantilever Kiwoong Kim and Soonchil Lee*, vol. J. Appl. Phys., pp. 1454225, 2002.
- [28] K. Aubin, M. Zalalutdinov, T. Alan, R.B. Reichenbach, R. Rand, A. Zehnder, J. Parpia, and H. Craighead, “Limit cycle oscillations in CW laser-driven NEMS,” *J. MEMS*, vol. 13, pp. 1018–1026, 2004.
- [29] T. Carmon, H. Rokhsari, L. Yang, T. J. Kippenberg, and K. J. Vahala, “,” *Phys. Rev. Lett.*, vol. 94, pp. 223902, 2005.
- [30] T. Corbitt, D. Ottaway, E. Innerhofer, J. Pelc, and N. Mavalvala, “,” *Phys. Rev. A*, vol. 74, pp. 21802, 2006.
- [31] T. Carmon and K. J. Vahala, “,” *Phys. Rev. Lett.*, vol. 98, pp. 123901, 2007.
- [32] Stav Zaitsev, Oded Gottlieb, and Eyal Buks, “Nonlinear dynamics of a microelectromechanical mirror in an optical resonance cavity,” *Nonlinear Dynamics (in press)*, *arXiv:1104.2235*, 2011.
- [33] Stav Zaitsev, Ashok K. Pandey, Oleg Shtempluck, and Eyal Buks, “Forced and self-excited oscillations of optomechanical cavity,” *Phys. Rev. E* 84, vol. 84, pp. 046605, 2011.
- [34] W. Riethmuller and W. Benecke, “Thermally excited silicon microactuators,” *IEEE Trans. Electron. Dev.*, vol. 35, pp. 758–762, 1988.
- [35] A. Michael and C.Y. Kwok, “Buckling shape of elastically constrained multi-layered micro-bridges,” *Sensors and Actuators A*, vol. 135, pp. 870–880, 2007.
- [36] David S. Ross, Antonio Cabal, David Trauernicht, and John Lebens, “Temperature-dependent vibrations of bilayer microbeams,” *Sensors and Actuators A*, vol. 119, pp. 53–543, 2005.
- [37] D. A. Rodrigues and A. D. Armour, “Amplitude noise suppression in cavity-driven oscillations of a mechanical resonator,” *Phys. Rev. Lett.*, vol. 104, pp. 053601, Feb 2010.
- [38] Hajime Okamoto, Takehito Kamada, Koji Onomitsu, Imran Mahboob, and Hiroshi Yamaguchi, “,” *Applied Physics Express*, vol. 2, pp. 062202, 2009.
- [39] Douglas W. Coffin and Frederick Bloom, “Elastica solution for the hygrothermal buckling of a beam,” *International Journal of Non-Linear Mechanics*, vol. 34, pp. 935–947, 1999.
- [40] W. Fang and J.A. Wickert, “Post buckling of micro-machined beams,” *J. Micromech. Microeng.*, vol. 4, pp. 116–122, 1994.
- [41] J. M. Gere and S. P. Timoshenko, *Mechanics of Materials*, PWS, Boston, MA, 1997.
- [42] Joseph J Talghader, “Thermal and mechanical phenomena in micromechanical optics,” *J. Phys. D: Appl. Phys.*, vol. 37, pp. R109–R122, 2004.
- [43] A. Ettouhami, A. Essaid, N. Ouakrim, L. Michel, and M. Limou.D, “Thermal buckling of silicon capacitive pressure sensor,” *Sensors and Actuators A*, vol. 57, pp. 167–171, 1996.
- [44] Matthew McCarthy, Nicholas Tiliakos, Vijay Modi, and Luc G. Frechette, “Thermal buckling of eccentric micro-

- fabricated nickel beams as temperature regulated nonlinear actuators for flow control,” *Sensors and Actuators A: Physical*, vol. 28, pp. 37–46, 2007.
- [45] Mahmood Bagheri, Menno Poot, Mo Li, Wolfram P. H. Pernice, and Hong X. Tang, “Dynamic manipulation of nanomechanical resonators in the high-amplitude regime and non-volatile mechanical memory operation,” *Nature Nanotechnology*, vol. 6, pp. 726–732, 2011.
- [46] D. Roodenburg, J. W. Spronck, H. S. J. van der Zant, and W. J. Venstra, “Buckling beam micromechanical memory with on-chip readout,” *Appl. Phys. Lett.*, vol. 94, pp. 183501, 2009.
- [47] A. H. Nayfeh, W. Kreider, and T. J. Anderson, “Investigation of natural frequencies and mode shapes of buckled beams,” *AIAA Journal*, vol. 33, pp. 1121–1126, June 1995.
- [48] W. E. Lawrence, M. N. Wybourne, and S. M. Carr, “Compressional mode softening and euler buckling patterns in mesoscopic beams,” *N. J. Phys.*, vol. 8, pp. 223, 2006.
- [49] David Blocher, Alan T. Zehnder, Richard H. Rand, and Shreyasi Mukerji, “Anchor deformations drive limit cycle oscillations in interferometrically transduced mems beams,” *Finite Elem. Anal. Des.*, vol. 49, pp. 52–57, Feb. 2012.
- [50] A. W. Snyder and J. D. Love, *Optical waveguide theory*, Springer, 1983.
- [51] A. W. Snyder and J. D. Love, *Optical Waveguide Theory*, Chapman and Hall, 1983.
- [52] Resonance Mode Expansions L. Poladian and 29632975 (1996). Exact Solutions for Nonuniform Gratings, *Phys. Rev. E* 54, “L. poladian,” *Phys. Rev. E*, vol. 54, pp. 2963–2975, 1996.
- [53] Youxin Mao, Shoude Chang, Sherif Sherif, and Costel Flueraru, “Graded-index fiber lens proposed for ultra-small probes used in biomedical imaging,” *Appl. Opt.*, vol. 46, pp. 5887–5894, 2007.
- [54] A. Schliesser, P. DelHaye, N. Nooshi, K. J. Vahala, and T. J. Kippenberg, “Radiation pressure cooling of a micromechanical oscillator using dynamical backaction,” *Phys. Rev. Lett.*, vol. 97, pp. 243905, 2006.
- [55] Ashok Kumar Pandey, Oded Gottlieb, Oleg Shtempluck, and Eyal Buks, “Performance of an AuPd micromechanical resonator as a temperature sensor,” *Appl. Phys. Lett.*, vol. 96, pp. 203105, 2010.
- [56] W. Fang and J. A. Wickert, “Determining mean and gradient residual stresses in thin films using micromachined cantilevers,” *J. Micromech. Microeng.*, vol. 6, pp. 301–309, 1996.
- [57] T. G. Leong, B. R. Benson, E. K. Call, and D. H. Gracias, “Thin film stress driven self-folding of microstructured containers,” *Small*, vol. 4, no. 10, pp. 1605–1609, Oct 2008.